Biomolecules and Biomedicine

ISSN: 2831-0896 (Print) | ISSN: 2831-090X (Online)

Journal Impact Factor® (2023): 3.1

CiteScore® (2023): 7.4
www.biomolbiomed.com | blog.biomolbiomed.com

SUPPLEMENTAL DATA

Zhang et al: MHC-I pathway predicts response to PD-1/PD-L1 blockade

The MHC-I-dependent neoantigen presentation pathway predicts response rate to PD-1/PD-L1 blockade

Yuchen Zhang[#], Chen Yang[#] , Yanchao Xu, Xiang Jiang, Jiajun Shi, Binghua Li[*], Decai Yu[*]

State Key Laboratory of Pharmaceutical Biotechnology, Division of Hepatobiliary and Transplantation Surgery, Department of General Surgery, Nanjing Drum Tower Hospital, The Affiliated Hospital of Nanjing University Medical School, Nanjing, China

*__Correspondence to__ Binghua Li lbhnju@163.com and Decai Yu: yudecai@nju.edu.cn

[#]Yuchen Zhang and Chen Yang equally contributed.

DOI: https://doi.org/10.17305/bb.2024.11069

Full article is available at the following link:
https://www.bjbms.org/ojs/index.php/bjbms/article/view/11069

Table S1. Full names, ORRs and patient numbers of the tumor types in the study.

Study Abbreviation	Study Name	ORR (%)	Patient number
ACC	Adrenocortical carcinoma	6	78
BLCA	Bladder Urothelial Carcinoma	18.4	407
BRCA	Breast invasive carcinoma	5.2	1006
CESC	Cervical squamous cell carcinoma and endocervical adenocarcinoma	19.8	285
GBM	Glioblastoma multiforme	8.8	155
HNSC	Head and Neck squamous cell carcinoma	14.8	494
KIPAN	Renal Cell Carcinoma	23.8	631
LIHC	Liver hepatocellular carcinoma	17.5	355
LUAD	Lung adenocarcinoma	17	506
LUSC	Lung squamous cell carcinoma	17.5	469
MESO	Mesothelioma	13	82
OV	Ovarian serous cystadenocarcinoma	10	205
PAAD	Pancreatic adenocarcinoma	0.2	169
PRAD	Prostate adenocarcinoma	7.5	493
READ	Rectum adenocarcinoma	24	138
SARC	Sarcoma	9.5	232
SKCM	Skin Cutaneous Melanoma	37	465
STES	Esophagogastric Carcinoma	9.9	590

TGCT	Testicular Germ Cell Tumors	0.2	143
UCEC	Uterine Corpus Endometrial Carcinoma	13.5	513
UVM	Uveal Melanoma	4.8	80

Table S2. Correlations between immune characteristics and objective response rate with anti-PD-1 or anti-PD-L1 therapy in 21 tumor types.

Immune Characteristics	**Spearman's rho**	**p value**
Leukocyte. Fraction	0.179	0.44
Stromal. Fraction	0.047	0.84
Intratumor. Heterogeneity	0.262	0.25
TIL. Regional. Fraction	0.378	0.23
Proliferation	0.231	0.31
Wound. Healing	0.263	0.25
Macrophage. Regulation	-0.034	0.89
Lymphocyte. Infiltration. Signature. Score	0.158	0.49
IFN. gamma. Response	-0.014	0.95
TGF. beta. Response	0.127	0.58
SNV. Neoantigens	**0.756**	**7.25E-05**
Indel. Neoantigens	**0.644**	**0.0029**
Silent. Mutation. Rate	**0.759**	**6.65E-05**
Nonsilent. Mutation. Rate	**0.749**	**9.29E-05**
Number.of.Segments	0.089	0.70

Fraction. Altered	0.062	0.79
Aneuploidy. Score	0.111	0.63
Homologous. Recombination. Defects	0.18	0.43
BCR. Evenness	0.235	0.31
BCR. Shannon	0.178	0.44
BCR. Richness	0.082	0.72
TCR. Shannon	0.095	0.68
TCR. Richness	0.11	0.64
TCR. Evenness	-0.142	0.54
CTA. Score	-0.007	0.98
Th1.Cells	-0.078	0.74
Th2.Cells	0.006	0.98
Th17.Cells	0.195	0.40
B.Cells. Memory	-0.131	0.57
B.Cells. Naive	-0.061	0.79
Dendritic. Cells. Activated	0.152	0.51
Dendritic. Cells. Resting	0.112	0.63
Macrophages.M0	0.069	0.77
Macrophages.M1	0.244	0.29
Macrophages.M2	-0.255	0.27
Mast.Cells. Activated	0.184	0.43
Mast.Cells. Resting	-0.439	0.047
Monocytes	-0.209	0.36

Neutrophils	0.198	0.39
NK.Cells. Activated	-0.041	0.86
NK.Cells. Resting	0.144	0.53
Plasma. Cells	0.154	0.51
T.Cells.CD4. Memory. Resting	-0.181	0.43
T.Cells.CD8	**0.449**	**0.041**
T.Cells. Follicular. Helper	0.294	0.20
T.Cells. Regulatory. Tregs	0.248	0.28
Lymphocytes	0.385	0.086
Neutrophils.1	0.198	0.39
Mast. Cells	-0.34	0.13
Dendritic. Cells	0.275	0.23
Macrophages	-0.414	0.062
TMB	**0.783**	**2.71E-05**
PD-L1	0.282	0.22
HLA-A	**0.509**	**0.018**
HLA-B	**0.637**	**0.0019**
HLA-C	**0.671**	**0.00088**
GO_ANTIGEN_PROCESSING_AND_ PRESENTATION_OF_ENDOGENOUS_ ANTIGEN	**0.722**	**0.00022**

*The indexes shown in bold are positively correlated with ORR.

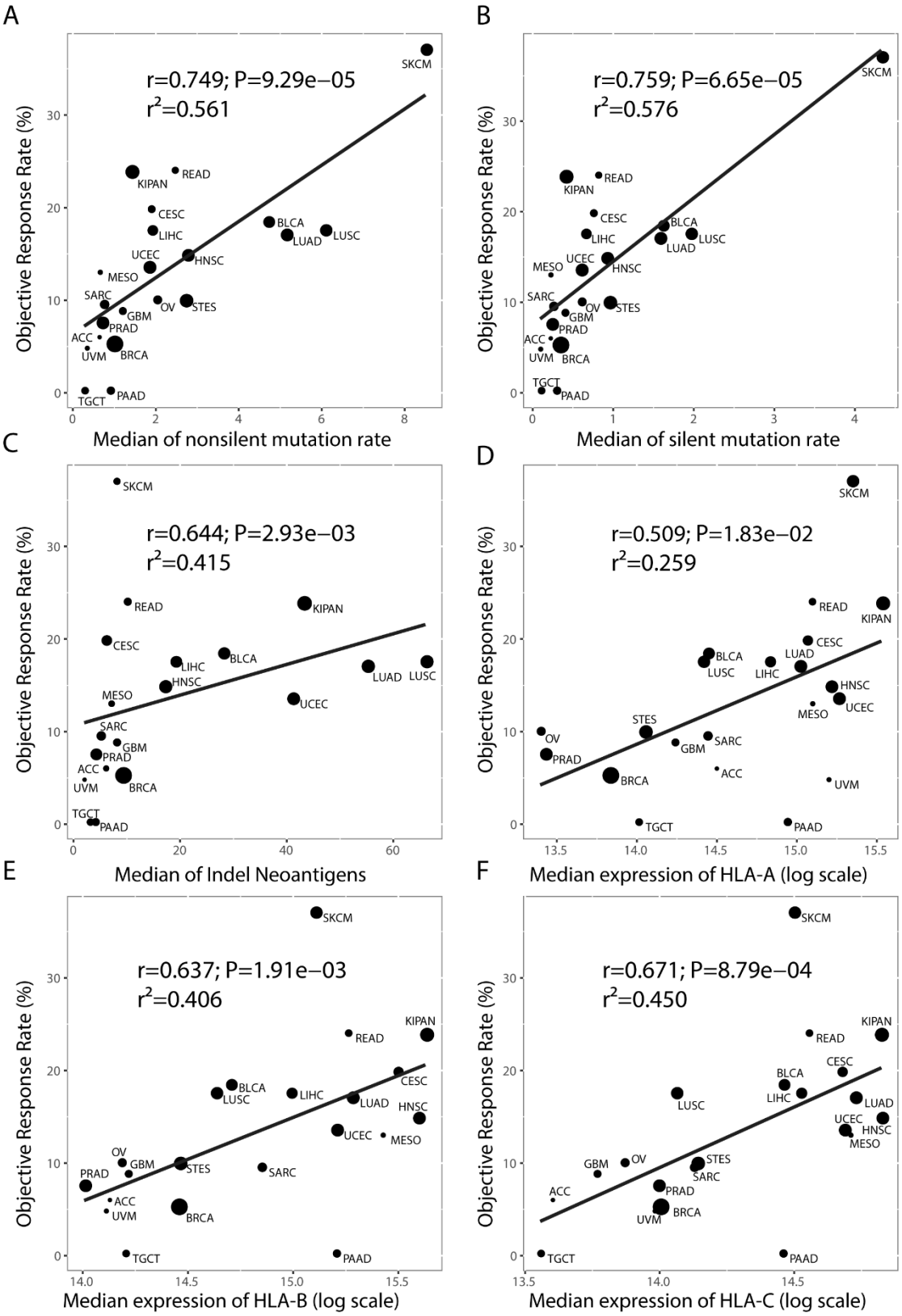

Figure S1. ORR-related immune characteristics. Correlation between ORR and nonsilent mutation rate (A), silent mutation rate (B), Indel Neoantigens (C), HLA-A (D), HLA-B (E) and HLA-C (F) across cancer types in TCGA dataset.

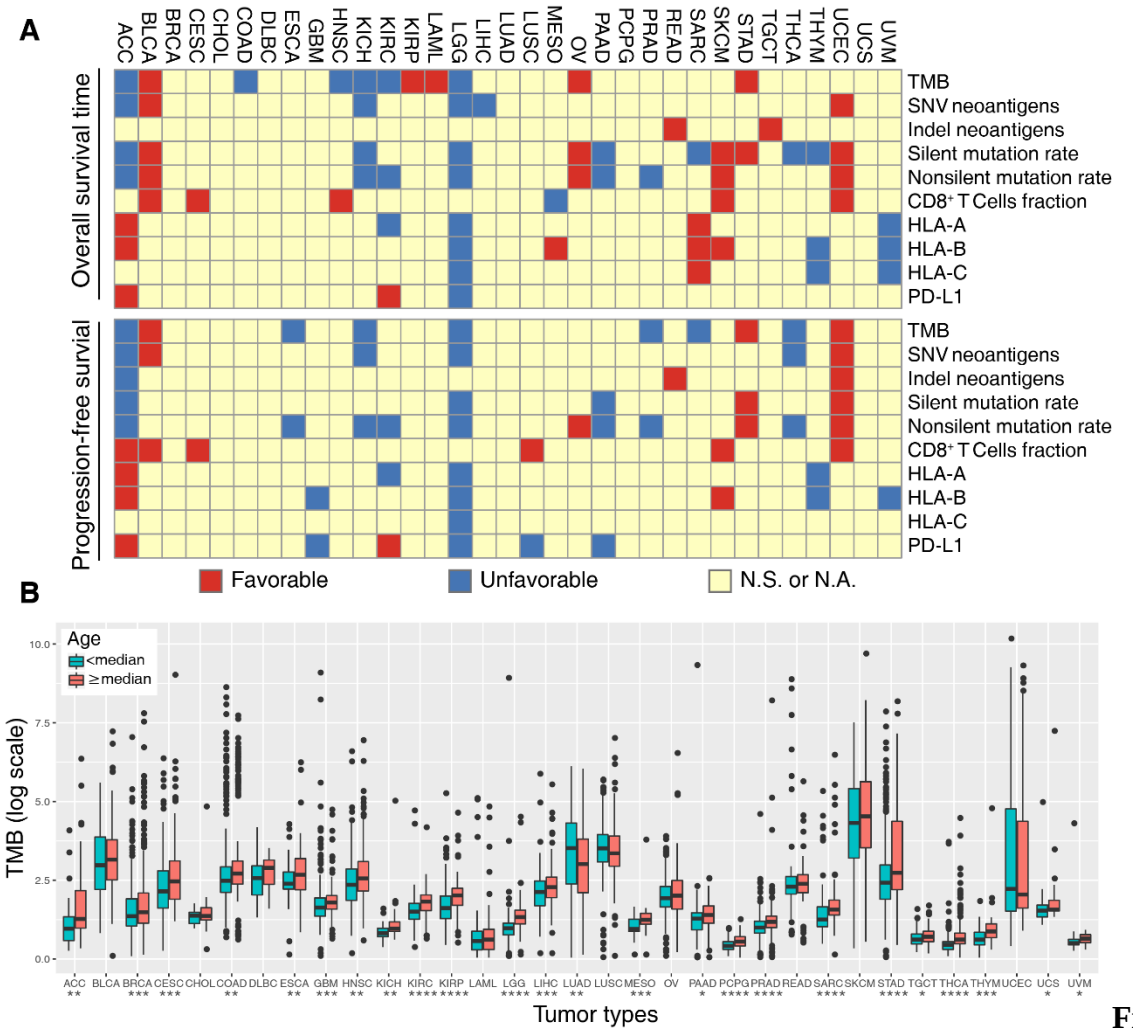

Figure S2. (A) Survival analysis of ORR-related immune characteristics. Upper panel: overall survival time; lower panel: progression-free survival. Red indicates favorable prognosis, and blue indicates unfavorable prognosis. (B) Pan-cancer analysis of TMB across cancers from TCGA. The median of age in a specific tumor type was used as a cutoff value for classification of the young and older group.

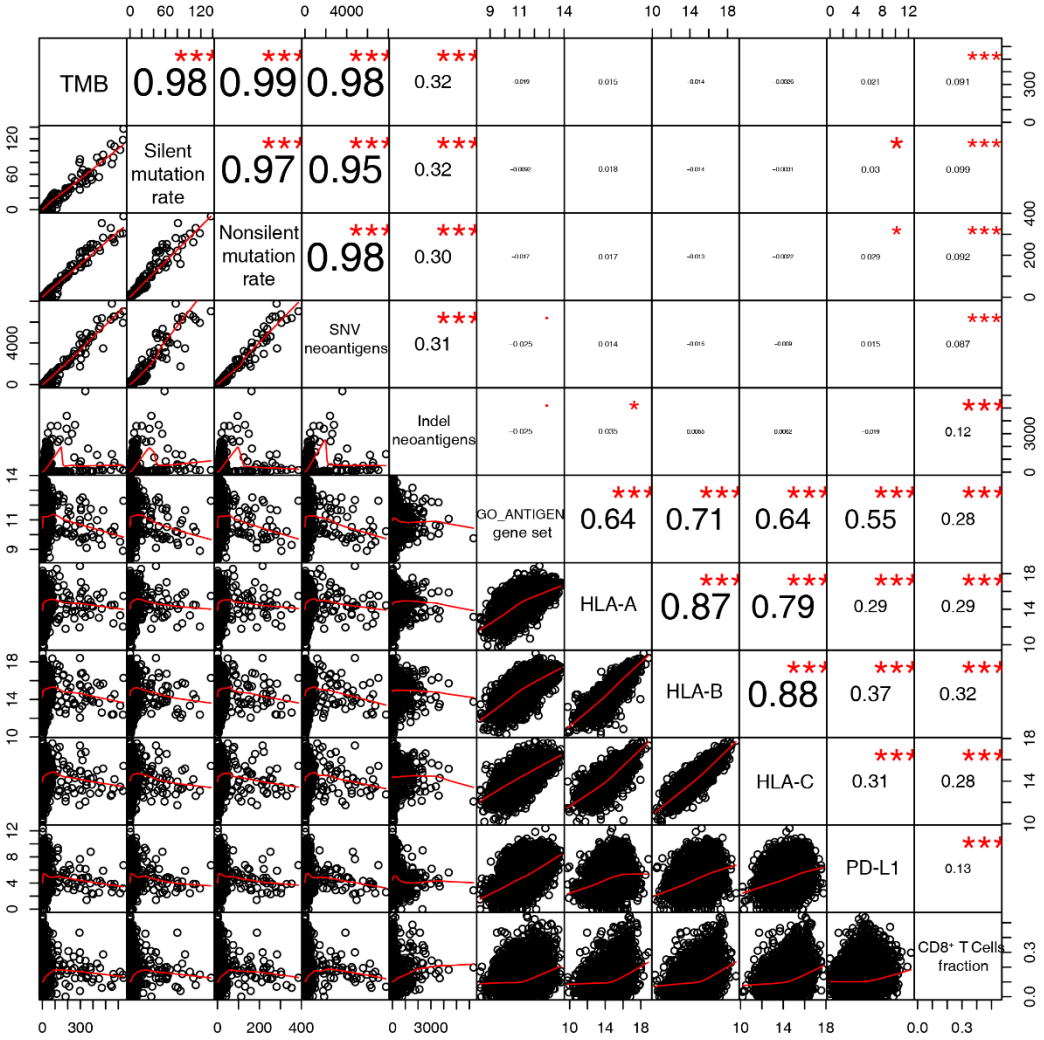

Figure S3. Correlation matrix of the ORR-related immune characteristics. The number indicates Spearman correlation coefficient. *, $P < 0.05$; **, $P < 0.01$; ***, $P < 0.001$.

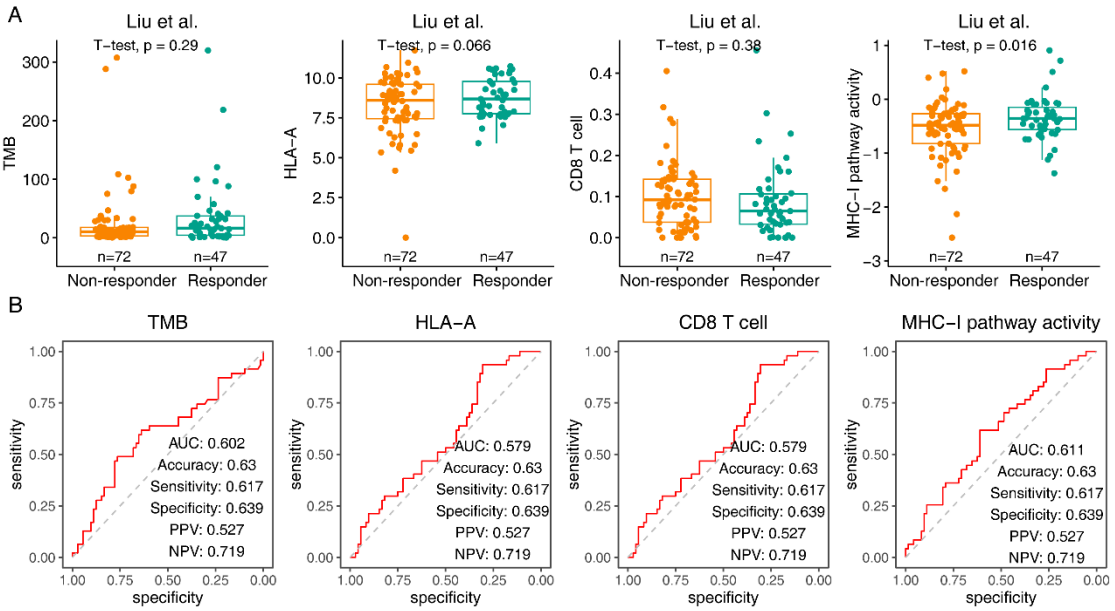

Figure S4. Validation of the predictive value of the MHC-I-dependent neoantigen presentation pathway in response to anti-PD-1 therapy in melanoma (Liu et al. cohort). (A) Boxplot comparing TMB, HLA-A expression, CD8+ T cell infiltration, and MHC-I pathway activity between anti-PD-1 therapy responders and non-responders. (B) ROC curve showing the predictive accuracy of TMB, HLA-A, CD8+ T cell infiltration, and MHC-I pathway activity for anti-PD-1 therapy response in the Liu et al. cohort.

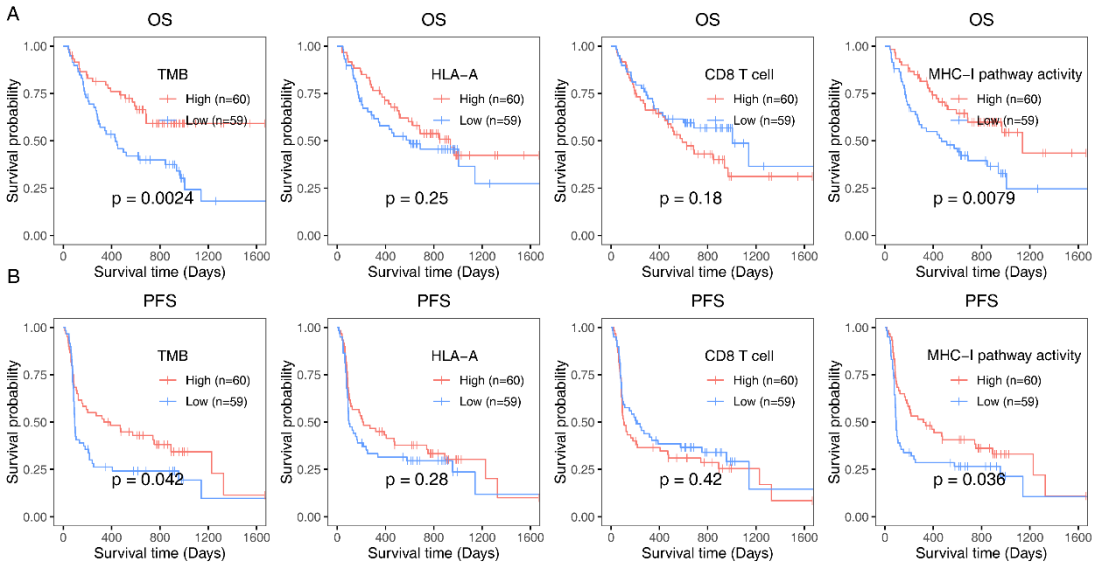

Figure S5. Correlation of the MHC-I-dependent neoantigen presentation pathway with survival in melanoma. Kaplan-Meier plots showing (A) OS and (B) PFS in the Liu et al. cohort, stratified into high and low groups (split by median) based on TMB, HLA-A expression, CD8+ T cell infiltration, and MHC-I pathway activity.